Gadolinium Effect at High-Magnetic-Field DNP: 70% ^{13}C Polarization of [U-^{13}C] Glucose Using Trityl

Capozzi, Andrea; Patel, Saket; Wenckebach, W. Thomas; Karlsson, Magnus; Lerche, Mathilde H.; Ardenkjær-Larsen, Jan Henrik

Published in:
Journal of Physical Chemistry Letters

Link to article, DOI:
10.1021/acs.jpclett.9b01306

Publication date:
2019

Document Version
Peer reviewed version

THE JOURNAL OF PHYSICAL CHEMISTRY Letters

Biophysical Chemistry, Biomolecules, and Biomaterials; Surfactants and Membranes

Gadolinium Effect at High Magnetic Field DNP: 70% ^{13}C Polarization of [U-^{13}C]glucose Using Trityl

Andrea Capozzi, Saket Patel, Tom Wenckebach, Magnus Karlsson, Mathilde Hauge Lerche, and Jan Henrik Ardenkjaer-Larsen

J. Phys. Chem. Lett., **Just Accepted Manuscript** • Publication Date (Web): 03 Jun 2019

Just Accepted

is published by the American Chemical Society. 1155 Sixteenth Street N.W., Washington, DC 20036

Gadolinium Effect at High Magnetic Field DNP: 70% ^{13}C Polarization of [U-^{13}C] Glucose Using Trityl

Andrea Capozzi,[1,] Saket Patel,[1] W. Thomas Wenckebach,[2,3] Magnus Karlsson,[1] Mathilde H. Lerche,[1] and Jan Henrik Ardenkjær-Larsen.[1,4]*

[1]Center for Hyperpolarization in Magnetic Resonance, Department of Health Technology, Technical University of Denmark, Building 349, 2800 Kgs Lyngby (Denmark)

[2]Paul Scherrer Institute, CH-5232 Villigen (Switzerland)

[3]National High Magnetic Field Laboratory, Gainesville, Florida (USA).

[4]GE Healthcare, Park Alle 295, 2605 Brøndby (Denmark)

Corresponding Author

*Andrea Capozzi, PhD

Technical University of Denmark

Ørsted Plads, Building 349, room 110

2800 Kgs. Lyngby

T: +45 45 25 53 27 ; Email: andcapo@dtu.dk

ABSTRACT

Herein, we show that the trityl Electron Spin Resonance (ESR) features, crucial for an efficient Dynamic Nuclear Polarization (DNP) process, are sample composition dependent. Working at 6.7 T and 1.1 K with a generally applicable DNP sample solvent mixture such as water:glycerol plus trityl, addition of Gd^{3+} lead to a dramatic increase of [U-^{13}C]glucose polarization from 37±4% to 69±3%. This is the highest value reported to date and comparable to what can be achieved on pyruvic acid. Moreover, performing ESR measurements at actual DNP conditions, we provide experimental evidence that gadolinium doping not only shortens the trityl electron spin-lattice relaxation time but also

modifies the radical g-tensor. The latter yielded a considerable narrowing of the ESR spectrum linewidth. Finally, in the frame of the spin temperature theory, we argue on how and within which boundaries these two phenomena can improve the DNP performances.

TOC GRAPHICS

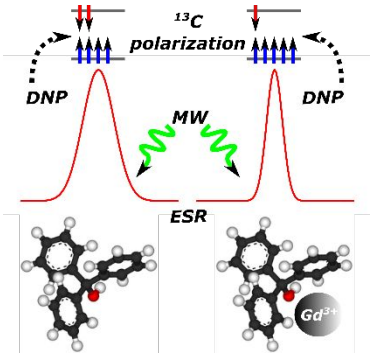

KEYWORDS: dDNP, gadolinium, glucose, hyperpolarization, LOD-ESR, trityl.

Hyperpolarization of nuclear spins via dissolution Dynamic Nuclear Polarization (dDNP)[1] has proven its great potential in enhancing the sensitivity of a broad variety of molecules, in particular for detection with ^{13}C Nuclear Magnetic Resonance (NMR) and Magnetic

Resonance Imaging (MRI).[2-3] Prior to dissolution, the microwave driven polarization transfer from the electron spins, in form of free radicals, to the nuclear spins of interest takes place in the solid state at cryogenic temperature (1 – 1.5 K) and moderate magnetic field (3.35 – 7 T).[4] Neat [1-^{13}C]pyruvic acid (PYR) doped with the trityl[a] free radicals has become the most studied sample because of [1-^{13}C]pyruvate's undisputed usefulness in biomedical applications,[5-7] the really high achievable carbon polarization (up to 70%)[8-10] and its relatively long relaxation time constant after dissolution.[11] Detailed studies for different trityl-based samples are scarcer, limiting the potential of other biologically interesting substrates. A crucial example is the so-called "gadolinium effect". At the broadly used dDNP field value (i.e. 3.35 T), admixture of small amounts of Gd^{3+} can double the polarization enhancement of neat [1-^{13}C]PYR/trityl samples, leading to 40% carbon polarization at optimal conditions.[12] Differently, increasing the magnetic field strength (4.6 – 7 T), where the same sample can reach ^{13}C polarization of 60 – 70 %,

[a] Discussion of other polarizing agents such as BDPA and TEMPO is beyond the scope of the present manuscript. To avoid confusion, we specify that all data, observation and comments taken from the literature are limited to the case of trityl.

almost negligible improvement or worsening of the DNP enhancement factor has been observed by adding Gd^{3+}.[8, 13-15] At 3.35 T, trityl based non-PYR DNP samples showed ^{13}C polarization gain as high as 4-folds[12, 16-19], but those samples did not excessively benefit from increasing the magnetic field strength.[20-22] At magnetic fields higher than 3.35 T, very little has been published on the effect of Gd^{3+}, or other lanthanides, on trityl based non-PYR DNP sample preparations. The behavior between different DNP sample preparations is often explained by changes in nuclear and electron relaxation parameters.[15] In particular, although the precise physical mechanism behind the "gadolinium effect" is still not fully understood, shortening of the electron spin-lattice relaxation time (T_{1e}) is the most acknowledged process to contribute to the nuclear polarization increase.[12, 17-19] Often, because of hardware limitations, ESR measurements tailored at understanding the process behind the "gadolinium effect" are performed at field strengths and/or temperatures deviating from the targeted DNP conditions.[16-19, 23] These experimental boundaries place severe restrictions on continuous efforts to better understand and improve the DNP process.

The purpose of this work was to measure the trityl main ESR features at high field DNP conditions (6.7 T) and cryogenic temperatures (1.1 K) to investigate the mechanism behind Gd-doping. Using a purpose built Longitudinal Detection (LOD) ESR probe,[24] we could compare the properties of trityl embedded in a generally applicable sample matrix (glycerol-water) for [U-^{13}C,d_7]-D-glucose polarization, to the well-studied sample of trityl in neat [1-^{13}C]PYR. The choice of glucose was driven by a growing interest in the hyperpolarization community for this substrate, which is central for energy metabolic studies in all cells. Also, the use of glucose has been limited so far by the relatively low achievable carbon polarization, even at high field.[20] In particular, we aimed at investigating if T_{1e} reduction was the only parameter affected by Gd^{3+} doping and why, for the same trityl radical concentration and experimental conditions, neat PYR samples outperform other ^{13}C-labeled substrates at high magnetic field. We will discuss our results in the frame of spin temperature theory and the DNP mechanism known as Thermal Mixing (TM).[4, 25]

In a recent publication, Ardenkjær-Larsen at al. investigated the optimal AH111501 trityl concentration as a function of the magnetic field strength to achieve efficient DNP on neat [1-^{13}C]PYR.[13] At 6.7 T the optimum turned out to be 30 mM. We chose [1-^{13}C]PYR plus 30 mM AH111501 trityl as benchmark sample formulation for our study (from now onward referred as *PYR_sample*). The corresponding DNP sweep overlaid to the radical LOD-ESR spectrum and T_{1e} measurements are reported in Figure 1, panel A and B, respectively. The *PYR_sample* showed a somewhat asymmetric ESR spectrum centered at ω_0 = 187.99 GHz with full-width at half-maximum (FWHM) of 84±2 MHz well matched to the ^{13}C Larmor frequency (71.8 MHz). At this low temperature, the trityl radical g-tensor appeared rhombic (g_{xx} = 2.00332, g_{yy} = 2.00311, g_{zz} = 2.00237; see Supporting Information, Figure S1) rather than axial, as reported previously by Lumata et al. for measurements performed at 100 K.[16] The DNP sweep reflected well the asymmetry of the ESR spectrum, showing a slightly sharper negative lobe and zero crossing very close to ω_0. The T_{1e} measured 400±2 ms, less than half of the value previously reported at 3.35 T and 1.2 K for a sample of neat [1-^{13}C]PYR doped with 15 mM trityl (approx. 1000 ms).[12] At the optimum microwave irradiation frequency (i.e. 187.94 GHz), corresponding

to the DNP positive maximum, 70±5% carbon polarization was achieved with a buildup time constant of 1200±50 s (see Supporting Information, Figure S2). Moreover, modulation of the microwave frequency had no effect on the buildup time and DNP enhancement indicating that the *PYR_sample* was characterized by fast and efficient electron spectral diffusion. The relatively short T_{1e} of the *PYR_sample* was not merely a radical concentration effect. For a sample containing 15 mM trityl only we measured a T_{1e} of 430±3 ms (see Supporting Information, Figure S3).

The same concentration of AH111501 trityl radical (i.e. 30 mM) was used in the preparation of a sample containing 2 M [U-^{13}C,d_7]-D-glucose in glycerol:water 50:50 (v:v) (from now onward referred as *GLU0_sample*). For this sample, the maximum achievable DNP enhancement was lower than the *PYR_sample*. At the optimum microwave irradiation frequency (i.e. 187.93 GHz), corresponding to the DNP positive maximum, 37±4% carbon polarization was achieved with a buildup time constant of 1330±50 s (see Table 1). Also in this case modulation of the microwave frequency had no effect. The *GLU0_sample* T_{1e} was 2.5 times longer and the LOD-ESR spectrum/^{13}C DNP sweep 20

% broader than the *PYR_sample* (see Figure 1, panel C and D, respectively). Indeed, the sample matrix composition modified the radical g-tensor that showed even more evident rhombic nature (g_{xx} = 2.00354, g_{yy} = 2.00305, g_{zz} = 2.00223; see Supporting Information, Figure S4). The different glassing sample matrix composition can also justify the 925±5 ms long T_{1e} since the phonon spectral distribution, at the origin of the electron spin-lattice relaxation in the solid-state at this low temperature, depends on the stiffness and density of the latter.[4]

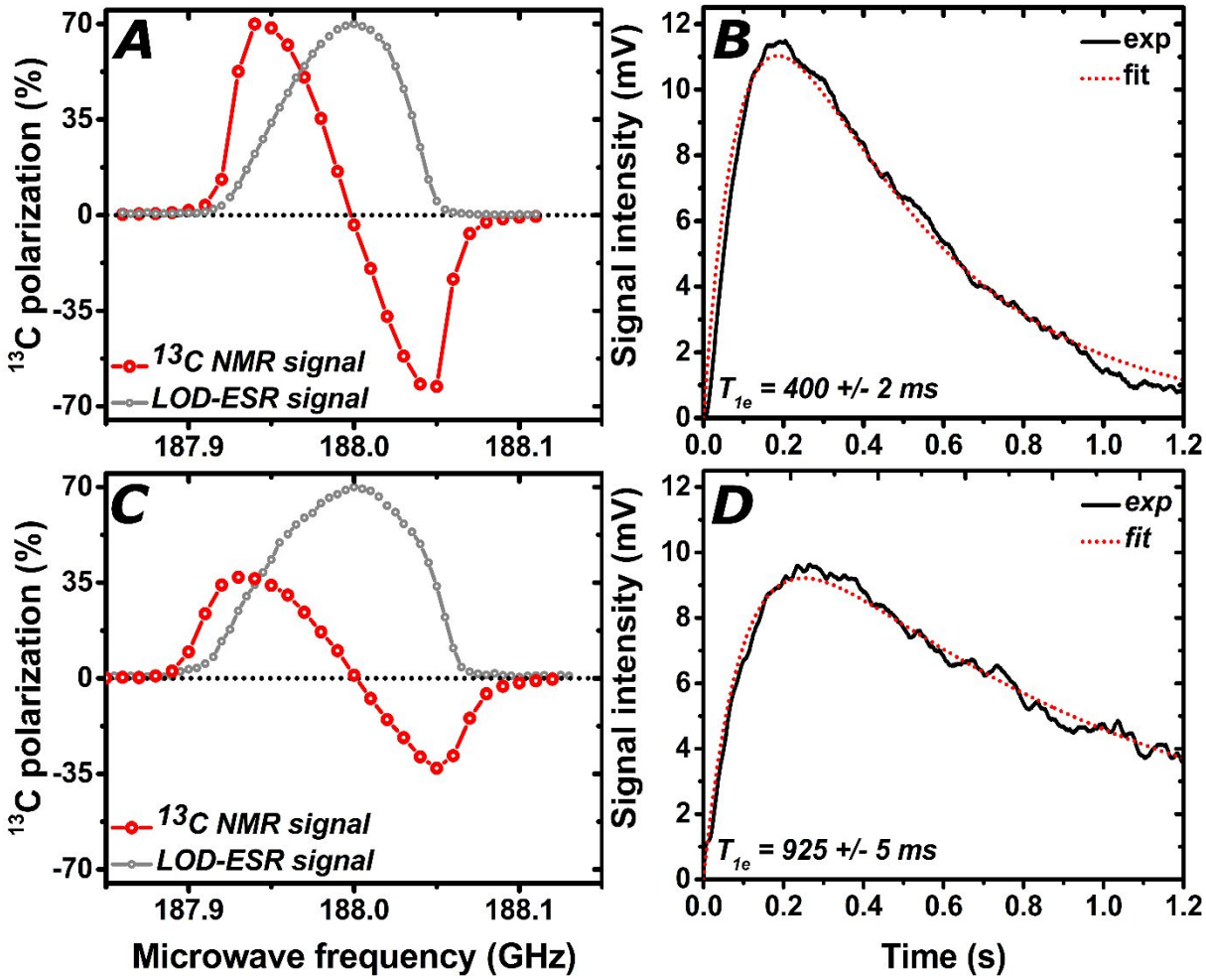

Figure 1 LOD-ESR spectrum overlaid with ^{13}C DNP sweep and T_{1e} measurement at 6.7 T and 1.1 K for neat [1-^{13}C]pyruvic acid (PYR) with 30 mM trityl (panel **A** and **B**) and 2 M [U-^{13}C,d_7]-D-glucose in glycerol:water 50:50 (v:v) with 30 mM trityl (panel **C** and **D**). The ESR spectrum intensity was maximized according to the panel dimension.

The longer T_{1e} of trityl dissolved in glycerol:water and glucose, compared to neat PYR at 6.7 T, encouraged us to investigate the effect of Gd^{3+} doping at different concentrations,

i.e. [Gd^{3+}] = 0.5 mM, 1 mM, 2 mM, 4 mM and 8 mM (from now onward the different glucose samples will be referred as *GLU[Gd^{3+}]_sample*). Already at 0.5 mM Gd^{3+} the T_{1e} dropped to 538±19 ms. As one would expect in a system containing a slow relaxing spin species (i.e. the trityl) and a dilute fast relaxing spin species (i.e. the Gd^{3+}), the spin-lattice relaxation rate ($1/T_{1e}$) increased linearly with the Gd^{3+} concentration (see Figure 2 panel B).[4, 26-27] Only the *GLU8_sample* deviated from this trend suggesting that at 8 mM Gd^{3+} concentration the interaction between the fast relaxing spins themselves was not negligible. Surprisingly, we also observed a narrowing of the ESR spectra especially on the high frequency hand side: the FWHM decreased to 85±2 MHz for the *GLU0.5_sample* and continued monotonically to 65±2 MHz for the *GLU8_sample* (see Figure 2 panel A and panel D); the g-tensor gradually evolved from rhombic to axial and the principal values obtained by Lumata et al from measurements performed at 100 K[16] resulted in a very good fit for the *GLU8_sample* ESR spectrum (see Supporting Information, Figure S4). The origin of the narrowing is still not clear. Less efficient spectral diffusion, caused by T_{1e} shortening, can generate some narrowing of the ESR spectrum due to more difficult electron spins saturation at the extreme edges of the latter. Nevertheless, while trityl $1/T_{1e}$

increases linearly upon Gd^{3+} doping of the glucose samples, the ESR FWHM appears to reach a minimum of approx. 60 MHz. Therefore, the contribution of a different phenomenon involving a modification of the radical g-anisotropy may be involved. To clarify this point, more extensive work involving simulations of the influence spectral diffusion on the LOD signal will be required.

The glucose samples series showed ^{13}C DNP sweeps with increasingly closer maxima as a function of the Gd^{3+} concentration (see Figure 2, panel C). This characteristic behavior was reported previously[17] and a purely T_{1e} reduction could justify it.[25, 28-29] Nevertheless, in our case the DNP sweeps consistently followed the ESR spectra appearance modification: besides the narrowing, they became more and more asymmetric revealing a growing negative enhancement for increasing Gd^{3+} concentration. All concerned numerical values are summarized in columns 2 to 5 of Table 1; data for individual samples are reported in Supporting Information, Figure S5 and S6.

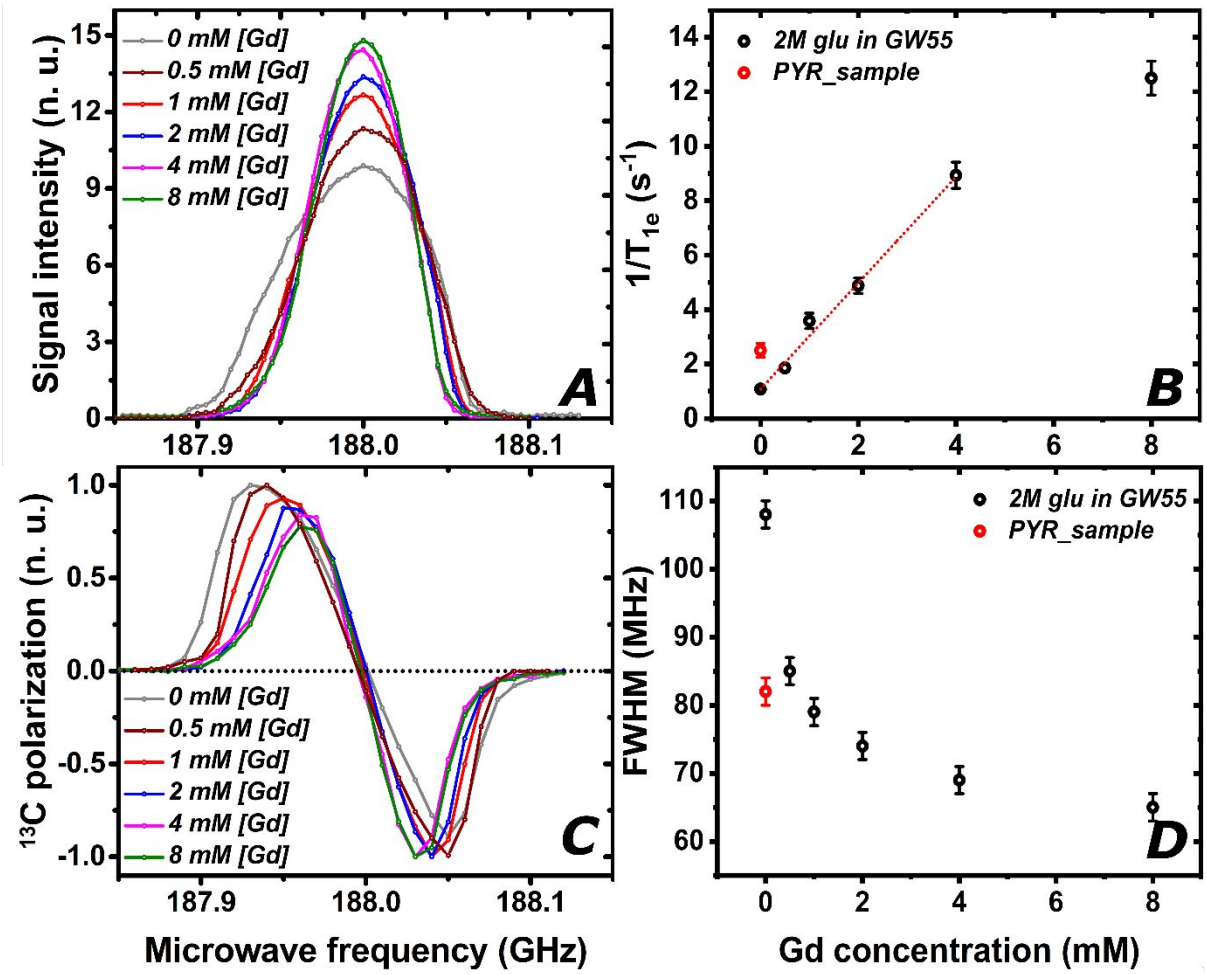

Figure 2 Effect of adding increasing concentrations of Gd^{3+} (color coded) to a 2 M [U-^{13}C,d_7]-D-glucose in glycerol:water 50:50 (v:v) sample doped with 30 mM trityl, at 6.7 T and 1.1 K. LOD-ESR spectra with integral value normalized to 1 (panel **A**). Electron spin-lattice relaxation rate; experimental points are represented by the black circles, while the dotted red curve shows a linear fit (panel **B**). DNP microwave sweeps (panel **C**). Measured FWHM (panel **D**). In panel **B** and **D** values for the *PYR_sample* have been added for comparison (red circles).

Gadolinium doping had a strong effect on the ^{13}C spin polarization of the glucose samples. At 0.5 mM Gd^{3+} concentration the nuclear spin polarization increased from 37±4% to 59±4%; the *GLU1_sample* achieved the maximum value (i.e. 69±3 %) and for higher Gd^{3+} concentration the polarization started to decrease (see Figure 3, panel A). Moreover, the buildup time constant (T_b) remained basically unchanged (approx. 1400 s) for all measured Gd^{3+} concentrations except for the *GLU8_sample* where a longer T_b was measured (see Figure 3, panel B). Solid-state polarization values and buildup time constants are reported in column 6 and 9 of Table 1.

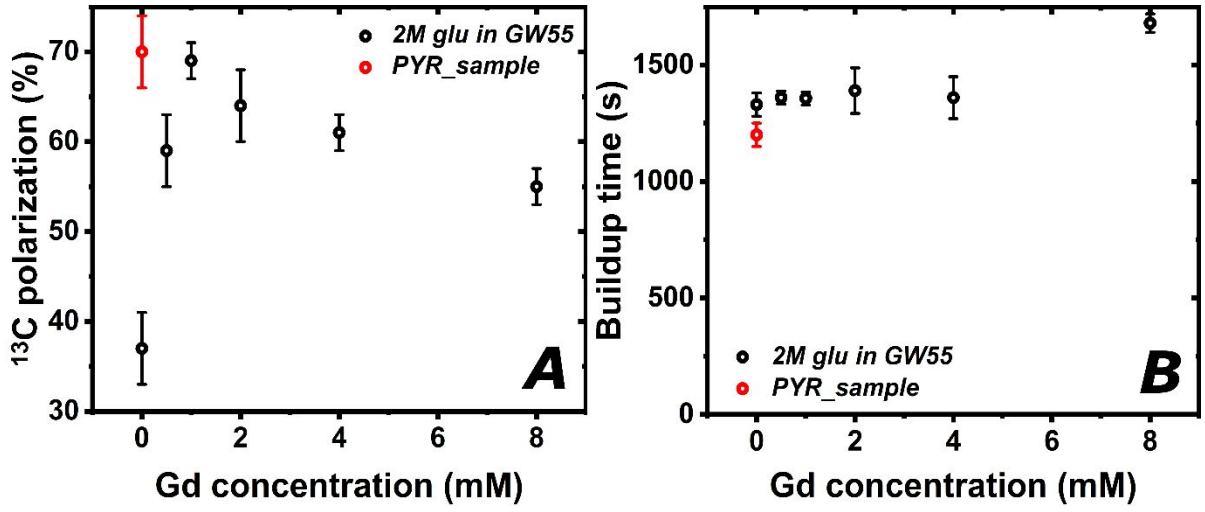

Figure 3 Solid-state ^{13}C polarization (panel **A**) and buildup time constant (panel **B**) as a function of the Gd^{3+} concentration in the glucose samples series (black circles) and the *PYR_sample* (red circle). For each sample the polarization was measured at best microwave irradiation conditions.

Our results show a strong correlation between the maximum achievable carbon polarization on one side and two trityl electron spin parameters on the other: T_{1e} and FWHM. Indeed, it is interesting to notice that [U-^{13}C,d_7]-D-glucose could reach a solid-state polarization value similar to the one achieved by the *PYR_sample* (i.e. 70%) when Gd^{3+} doping modified the aforementioned trityl radical parameters to match the ones observed in a pyruvic acid matrix (see position of red circles in Figure 3 panel B and D). According to the TM model and spin temperature interpretation of the DNP mechanism, within the correct boundaries, a reduction of both parameters can increase the maximum achievable nuclear polarization. To qualitatively clarify this point, it is useful to look at the analytical stationary solution of the extended Provotorov equations for the inverse electron non-Zeeman spin temperature $\beta_{NZ} = \hbar/k_B T_{NZ}$. This is available in the high temperature approximation,[25] where it is found to be

$$\frac{\beta_{NZ}}{\beta_L} = -\frac{2W_g(\omega)T_{1e}\omega_0(\omega-\omega_0)}{2W_g(\omega)T_{1e}\left[(\omega-\omega_0)^2+D^2\right]+D^2} \quad (1)$$

and

(2)

$$\lim_{s\to\infty}\frac{\beta_{NZ}}{\beta_L} = -\frac{\omega_0(\omega-\omega_0)}{(\omega-\omega_0)^2+D^2}$$

Here $\beta_L = \hbar/k_B T_L$ is the inverse lattice temperature, ω the microwave irradiation frequency; D^2 the second moment of the ESR spectrum related to its linewidth; $W_g(\omega)$ the rate of transitions induced by the microwaves and $s = W_g(\omega)T_{1e}$ the saturation parameter. As far as the ^{13}C Larmor frequency is smaller than the width of the ESR line, narrowing of the latter (i.e. smaller D) reduces the energy that can be stored in the non-Zeeman reservoir yielding directly to higher β_{NZ} that will eventually be transferred to the nuclei increasing their polarization enhancement. It is easy to see that when a strong microwave field is applied ($s>>1$), Eq. (2) has maxima $\pm\omega_0/2D$ at $\omega = \omega_0 \pm D$. If the ESR line becomes too narrow, the thermal contact between the electron non-Zeeman and nuclear Zeeman reservoirs decreases and the nuclear polarization is expected to drop.

Understanding the effect of T_{1e} shortening on the nuclear polarization is not as straightforward as for the ESR linewidth. Eq. (1), or its generalization beyond the high temperature approximation,[29] represents an ideal case where the nuclei can relax to the

lattice only via the electron non-Zeeman reservoir. In that case shortening T_{1e} is equivalent to reduce the microwave power, thus the saturation factor *s*. The consequence is a reduction of β_{NZ} and eventually a drop of the nuclear polarization.[30] Differently, if the system presents nuclear leakage (relaxation pathways different from the coupling to the electron non-Zeeman reservoir), a moderate reduction of T_{1e} can be beneficial. Indeed, the rate at which β_{NZ} is achieved depends on T_{1e} and shortening of the latter can make leakage relatively less important. [25]

The already short T_{1e} for the *PYR_sample* at 6.7 T can, at least partially, explain why addition of Gd^{3+} to DNP samples composed by neat [1-^{13}C]PYR plus trityl has a negligible effect at magnetic field values higher than 3.35 T.[8, 10, 14] At dDNP temperatures, the T_{1e} of trityl dissolved in a glassing matrix is dominated by the Orbach and direct process.[31] The Orbach process requires a hitherto unidentified excited state of the radical and involves two phonon modes coupling the two spin states to that excited state. The resulting relaxation rate is independent of the ESR frequency (ω_{oS}), but depends exponentially on the ratio between the ground state – excited state energy difference (ω_a)

and lattice temperature (T_L) such as $^{1}/_{T_{1e,Orb}} \sim (\omega_a)^3 / \left(e^{\hbar\omega_a / k_B T_L} - 1\right)$, where $\hbar$ and k_B are Planck's constant and Boltzman factor. Differently, the direct process involves only one phonon mode and its rate depends strongly on ω_{oS}, while being independent on the temperature under typical DNP conditions: $^{1}/_{T_{1e,dir}} \sim (\omega_{0S})^5 coth\left(\hbar\omega_{0S}/2k_B T_L\right)$.[25, 32] Thus, one would expect the Orbach process to prevail at low magnetic field, because more phonon modes can participate to the radical relaxation, and the direct process to provide a stronger contribution at high magnetic field. Our observation is in good agreement with Lumata et al.[16] They reported no difference for the T_{1e} of trityl between 9.5 GHz and 95 GHz, while a considerable reduction of the latter was measured at 240 GHz.

For the glucose samples we cannot exclude a priori some nuclear leakage (e.g. paramagnetic impurities like O_2 or trityl radical clusters), so up to 1 mM of Gd^{3+} concentration the reduction of the two radical parameters discussed above both improve the glucose polarization. Determining whether T_{1e} shortening or ESR line narrowing is more crucial in enhancing the glucose ^{13}C polarization in the range 0 – 1 mM of Gd^{3+} doping will need further investigation and is beyond the scope of the present work. For

higher concentrations, the DNP enhancement decreases mainly because of the drastic reduction of T_{1e} that prevents efficient ESR line saturation working at constant microwave power.

$[Gd^{3+}]$ (mM)	T_{1e} (ms)	ESR FWHM (MHz)	DNP maxima delta (MHz)	$\varepsilon_+/\varepsilon_-$	SS T_b (s)	LS T_1 (s)	LS pol (%)	SS pol (%)
0	925±4	108±2	120±5	1.124	1330±50	19.2±0.2	22±2	37±4
0.5	538±19	85±2	110±5	1.010	1368±28	19.2±0.1	35±2	59±4
1	279±11	79±2	90±5	0.930	1357±58	19.1±0.1	41±1	69±3
2	205±6	74±2	90±5	0.877	1390±98	19.0±0.2	38±2	64±4
4	112±3	69±2	70±5	0.796	1360±90	18.7±0.2	36±1	61±2
8	80±2	65±2	70±5	0.770	1680±40	17.4±0.3	31±2	55±2

Table 1 ^{13}C spin polarization of [U-$^{13}C_6$-d_7]-D-glucose at increasing Gd^{3+} concentrations. In solid state at 6.7 T and 1.1 K (SS pol) and 10 s after dissolution in 40 mM phosphate buffer pH 7.3, at 9.4 T and 50 °C (LS pol). **SS T_b** solid-state polarization build-up time constant. **LS T_1** Liquid state relaxation constant. **LS pol** liquid state polarization measured at 50 °C and 9.4 T 10 s after dissolution. **SS pol** solid-state polarization, back calculated given the liquid state relaxation constant and the sample transfer time from polarizer to NMR magnet.

The liquid-state ^{13}C polarization, measured in a 9.4 T vertical NMR magnet 10 s after dissolution and transport, nicely followed the trend of the solid-state values (see Table 1). To better visualize the strong carbon polarization enhancement achieved via Gd^{3+} doping, we report in Figure 4 the solid-state polarization buildup and liquid-state relaxation for the *GLU0_sample* and the *GLU1_sample*. Addition of 1 mM Gd^{3+} allowed us to achieve 41±1% liquid-state ^{13}C polarization, the highest value reported to date. Moreover, the liquid-state nuclear T_1 remained unchanged within the experimental errors (19.2±0.2 s). Liquid-state polarization and relaxation time constant values of the other glucose samples are reported in Table 1 columns 7 and 8.

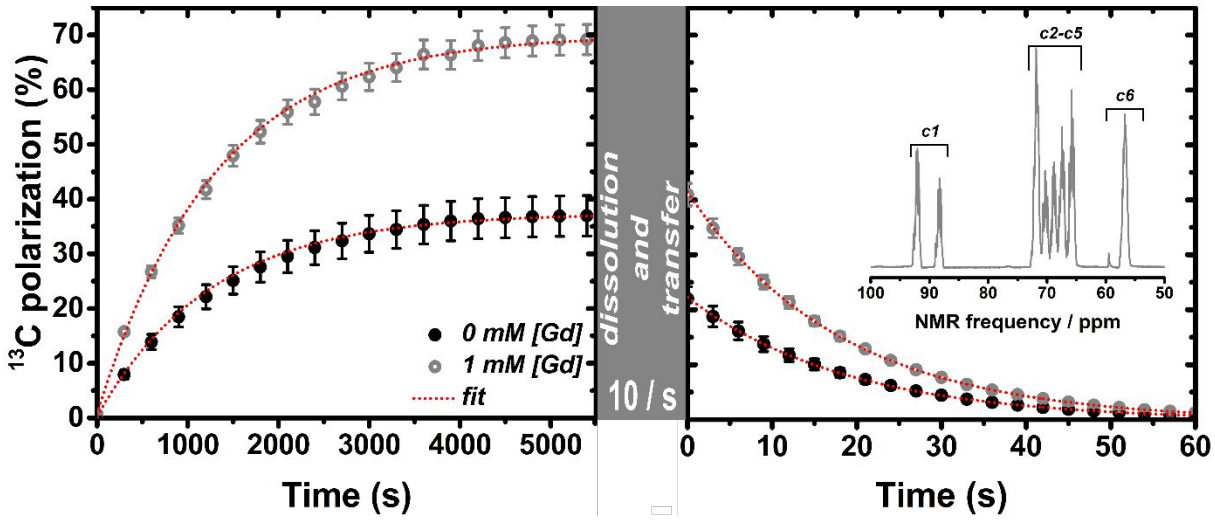

Figure 4 ^{13}C solid-state polarization at 6.7 T and 1.1 K (left panel) and relaxation after dissolution at 9.4 T and 313 K (right panel) of *GLU0_sample* (filled black circles) and *GLU1_sample* (open grey circles). The

middle panel indicates the 10 s sample transfer time from solid to liquid-state; the inset of the right panel shows the hyperpolarized ^{13}C glucose NMR spectrum.

It is very clear from this study that the sample matrix has a profound impact on the features of the trityl radical. The *PYR_sample* at high magnetic field is a "lucky" combination of these properties yielding ^{13}C polarization as high as 70%. Indeed, at 6.7 T and 1.1 K, the measured T_{1e} of trityl in a neat frozen PYR matrix was less than half of what it was in a glycerol/water mixture and the FWHM was 20 % narrower. When glycerol/water was employed as glassing solvent Gd^{3+} addition was used to fine tune the radical properties and significantly increase the glucose ^{13}C DNP enhancement matching the polarization value achieved by [1-^{13}C]pyruvic acid. The gadolinium not only decreased the trityl T_{1e}, as expected, but also generated a narrowing of the ESR spectrum.

ASSOCIATED CONTENT

This material is available free of charge via the Internet at http://pubs.acs.org.

- Experimental methods
- Additional results

AUTHOR INFORMATION/ CORRESPONDING AUTHOR

*Andrea Capozzi, PhD

Technical University of Denmark

Department of Health Technology

Ørsted Plads, Building 349, room 110

2800 Kgs. Lyngby

T: +45 45 25 53 27

Email: andcapo@dtu.dk

ORCID: 0000-0002-2306-9049

NOTES

The authors declare no conflict of interest.

ACKNOWLEDGMENT

We thank Dr Jacques van der Klink and Dr Olivier Ouari for fruitful discussions. The research leading to these results has received funding from the Danish National Research Foundation (DNRF124); the European Union's Horizon 2020 research and innovation programme under the Marie Sklodowska-Curie grant agreement no. 713683 (COFUNDfellowsDTU).

REFERENCES

1. Ardenkjaer-Larsen, J. H.; Fridlund, B.; Gram, A.; Hansson, G.; Hansson, L.; Lerche, M. H.; Servin, R.; Thaning, M.; Golman, K. Increase in signal-to-noise ratio of > 10,000 times in liquid-state NMR. *P Natl Acad Sci USA* **2003,** *100* (18), 10158-10163.

2. Kurhanewicz, J.; Vigneron, D. B.; Brindle, K.; Chekmenev, E. Y.; Comment, A.; Cunningham, C. H.; DeBerardinis, R. J.; Green, G. G.; Leach, M. O.; Rajan, S. S.; Rizi, R. R.; Ross, B. D.; Warren, W. S.; Malloy, C. R. Analysis of Cancer Metabolism by Imaging Hyperpolarized Nuclei: Prospects for Translation to Clinical Research. *Neoplasia* **2011,** *13* (2), 81-97.

3. Lerche, M. H.; Jensen, P. R.; Karlsson, M.; Meier, S. NMR Insights into the Inner Workings of Living Cells. *Anal Chem* **2015,** *87* (1), 119-132.

4. Abragam, A.; Goldman, M. Principles of Dynamic Nuclear-Polarization. *Rep Prog Phys* **1978,** *41* (3), 395-467.

5. Nelson, S. J.; Kurhanewicz, J.; Vigneron, D. B.; Larson, P. E. Z.; Harzstark, A. L.; Ferrone, M.; van Criekinge, M.; Chang, J. W.; Bok, R.; Park, I.; Reed, G.; Carvajal, L.; Small, E. J.; Munster, P.; Weinberg, V. K.; Ardenkjaer-Larsen, J. H.; Chen, A. P.; Hurd, R. E.; Odegardstuen, L. I.; Robb, F. J.; Tropp, J.; Murray, J. A. Metabolic Imaging of Patients with Prostate Cancer Using Hyperpolarized [1-C-13]Pyruvate. *Sci Transl Med* **2013,** *5* (198), 198ra108 1-10.

6. Golman, K.; in't Zandt, R.; Thaning, M. Real-time metabolic imaging. *P Natl Acad Sci USA* **2006,** *103* (30), 11270-11275.

7. Harris, T.; Eliyahu, G.; Frydman, L.; Degani, H. Kinetics of hyperpolarized C-13(1)-pyruvate transport and metabolism in living human breast cancer cells. *P Natl Acad Sci USA* **2009,** *106* (43), 18131-18136.

8. Yoshihara, H. A. I.; Can, E.; Karlsson, M.; Lerche, M. H.; Schwitter, J.; Comment, A. High-field dissolution dynamic nuclear polarization of [1-C-13]pyruvic acid. *Phys Chem Chem Phys* **2016,** *18* (18), 12409-12413.

9. Meyer, W.; Heckmann, J.; Hess, C.; Radtke, E.; Reicherz, G.; Triebwasser, L.; Wang, L. Dynamic polarization of C-13 nuclei in solid C-13 labeled pyruvic acid. *Nucl Instrum Meth A* **2011,** *631* (1), 1-5.

10. Johanneson, H.; Macholl, S.; Ardenkjaer-Larsen, J. H. Dynamic Nuclear Polarization of [1-C-13]pyruvic acid at 4.6 tesla. *J Magn Reson* **2009,** *197* (2), 167-175.

11. Friesen-Waldner, L.; Chen, A.; Mander, W.; Scholl, T. J.; McKenzie, C. A. Optimisation of dynamic nuclear polarisation of [1-(13)C] pyruvate by addition of gadolinium-based contrast agents. *J Magn Reson* **2012,** *223*, 85-9.

12. Ardenkjaer-Larsen, J. H.; Macholl, S.; Johannesson, H. Dynamic nuclear polarization with trityls at 1.2 K. *Appl Magn Reson* **2008,** *34* (3-4), 509-522.

13. Ardenkjaer-Larsen, J. H.; Bowen, S.; Petersen, J. R.; Rybalko, O.; Vinding, M. S.; Ullisch, M.; Nielsen, N. C. Cryogen-free dissolution dynamic nuclear polarization polarizer operating at 3.35 T, 6.70 T, and 10.1 T. *Magn Reson Med* **2019,** *81* (3), 2184-2194.

14. Jahnig, F.; Kwiatkowski, G.; Dapp, A.; Hunkeler, A.; Meier, B. H.; Kozerke, S.; Ernst, M. Dissolution DNP using trityl radicals at 7 T field. *Phys Chem Chem Phys* **2017,** *19* (29), 19196-19204.

15. Walker, S. A.; Edwards, D. T.; Siaw, T. A.; Armstrong, B. D.; Han, S. Temperature dependence of high field C-13 dynamic nuclear polarization processes with trityl radicals below 35 Kelvin. *Phys Chem Chem Phys* **2013,** *15* (36), 15106-15120.

16. Lumata, L.; Kovacs, Z.; Sherry, A. D.; Malloy, C.; Hill, S.; van Tol, J.; Yu, L.; Song, L. K.; Merritt, M. E. Electron spin resonance studies of trityl OX063 at a concentration optimal for DNP. *Phys Chem Chem Phys* **2013,** *15* (24), 9800-9807.

17. Lumata, L.; Merritt, M. E.; Malloy, C. R.; Sherry, A. D.; Kovacs, Z. Impact of Gd3+ on DNP of [1-C-13]Pyruvate Doped with Trityl OX063, BDPA, or 4-Oxo-TEMPO. *J Phys Chem A* **2012,** *116* (21), 5129-5138.

18. Niedbalski, P.; Parish, C.; Wang, Q.; Hayati, Z.; Song, L. K.; Martins, A. F.; Sherry, A. D.; Lumata, L. Transition Metal Doping Reveals Link between Electron T-1

Reduction and C-13 Dynamic Nuclear Polarization Efficiency. *J Phys Chem A* **2017,** *121* (48), 9221-9228.

19. Niedbalski, P.; Parish, C.; Wang, Q.; Kiswandhi, A.; Hayati, Z.; Song, L. K.; Lumata, L. C-13 Dynamic Nuclear Polarization Using a Trimeric Gd3+ Complex as an Additive. *J Phys Chem A* **2017,** *121* (27), 5127-5135.

20. Mishkovsky, M.; Anderson, B.; Karlsson, M.; Lerche, M. H.; Sherry, A. D.; Gruetter, R.; Kovacs, Z.; Comment, A. Measuring glucose cerebral metabolism in the healthy mouse using hyperpolarized C-13 magnetic resonance. *Sci Rep-Uk* **2017,** *7*.

21. Yoshihara, H. A. I.; Bastiaansen, J. A. M.; Karlsson, M.; Lerche, M. H.; Comment, A.; Schwitter, J. Myocardial fatty acid metabolism probed with hyperpolarized [1-13C]octanoate. *Journal of Cardiovascular Magnetic Resonance* **2015,** *17*.

22. Capozzi, A.; Patel, S.; Gunnarsson, C. P.; Marco-Rius, I.; Comment, A.; Karlsson, M.; Lerche, M. H.; Ouari, O.; Ardenkjaer-Larsen, J. H. Efficient Hyperpolarization of U-(13) C-Glucose Using Narrow-Line UV-Generated Labile Free Radicals. *Angewandte Chemie* **2019,** *58* (5), 1334-1339.

23. Niedbalski, P.; Parish, C.; Kiswandhi, A.; Fidelino, L.; Khemtong, C.; Hayati, Z.; Song, L. K.; Martins, A.; Sherry, A. D.; Lumata, L. Influence of Dy3+ and Tb3+ doping on C-13 dynamic nuclear polarization. *J Chem Phys* **2017,** *146* (1).

24. Capozzi, A.; Karlsson, M.; Petersen, J. R.; Lerche, M. H.; Ardenkjaer-Larsen, J. H. Liquid-State C-13 Polarization of 30% through Photoinduced Nonpersistent Radicals. *J Phys Chem C* **2018,** *122* (13), 7432-7443.

25. Wenckebach, W. T. *Essentials of Dynamic Nuclear Polarization*. Spindrift Publications, The Netherlands, 2016.

26. Bloembergen, N.; Purcell, E. M.; Pound, R. V. Relaxation Effects in Nuclear Magnetic Resonance Absorption. *Phys Rev* **1948,** *73* (7), 679-712.

27. Rakowsky, M. H.; More, K. M.; Kulikov, A. V.; Eaton, G. R.; Eaton, S. S. Time-Domain Electron-Paramagnetic-Resonance as a Probe of Electron-Electron Spin-Spin Interaction in Spin-Labeled Low-Spin Iron Porphyrins. *J Am Chem Soc* **1995,** *117* (7), 2049-2057.

28. Serra, S. C.; Filibian, M.; Carretta, P.; Rosso, A.; Tedoldi, F. Relevance of electron spin dissipative processes to dynamic nuclear polarization via thermal mixing. *Phys Chem Chem Phys* **2014,** *16* (2), 753-764.

29. Wenckebach, W. T. Dynamic nuclear polarization via thermal mixing: Beyond the high temperature approximation. *J Magn Reson* **2017,** *277*, 68-78.

30. Jannin, S.; Comment, A.; van der Klink, J. J. Dynamic Nuclear Polarization by Thermal Mixing Under Partial Saturation. *Appl Magn Reson* **2012,** *43* (1-2), 59-68.

31. Chen, H. J.; Maryasov, A. G.; Rogozhnikova, O. Y.; Trukhin, D. V.; Tormyshev, V. M.; Bowman, M. K. Electron spin dynamics and spin-lattice relaxation of trityl radicals in frozen solutions. *Phys Chem Chem Phys* **2016,** *18* (36), 24954-24965.

32. Abragam, A.; Bleaney, B. *Electron paramagnetic resonance of transition ions*. Clarendon P.: Oxford,, 1970; p xiv, 911 p.